The Canadian Mineralogist
Vol. 43, pp. 327-347 (2005)

FOLIATION DEVELOPMENT AND REACTION SOFTENING BY DISSOLUTION AND PRECIPITATION IN THE TRANSFORMATION OF GRANODIORITE TO ORTHOGNEISS, GLASTONBURY COMPLEX, CONNECTICUT, U.S.A.

ROBERT P. WINTSCH[§]

Department of Geological Sciences, Indiana University, Bloomington, Indiana 47405, U.S.A.

JOHN N. ALEINIKOFF

U.S. Geological Survey, Mail Stop 963, Denver, Colorado 80225, U.S.A.

KEEWOOK YI

Indiana University School of Dentistry, 415 Lansing Street, Indianapolis, Indiana 46202–2876, U.S.A.

ABSTRACT

Textures, microstructures, and patterns of chemical zoning in minerals in a granodioritic orthogneiss in the Glastonbury Complex, Connecticut, lead to the interpretation that foliation development was facilitated by retrograde hydration reactions in the presence of an aqueous fluid. Incomplete replacement of the metastable magmatic minerals K-feldspar + hastingsite + magnetite produced foliation-defining biotite + epidote + quartz. These reaction products did not replace K-feldspar – hastingsite interfaces; rather, either biotite or epidote replaced the amphibole, and plagioclase replaced K-feldspar. Biotite and epidote precipitated syntectonically in discrete layers that define the foliation in the orthogneiss, whereas quartz precipitated primarily in ribbons, further enhancing the fabric. Metastable REE-rich igneous titanite also dissolved, and was incompletely replaced by REE-poor, Al-bearing metamorphic titanite. The similar concentrations of the REE in epidote and titanite show that the REE released by titanite dissolution were precipitated locally as the allanite component in adjacent grains of epidote. The entire process was syntectonic, with most grains showing multiple overgrowths in the direction of extension as defined by stretched xenoliths. Sufficient U was present in the titanite overgrowths to allow SHRIMP dating of cores, mantles, and rims. These results suggest at least three retrograde Alleghanian events of growth in a span of ~30 m.y. Thus the dissolution – transportation – precipitation process not only describes the reaction mechanism but also leads to the redistribution of reaction products into nearly monomineralic layers, thus contributing to metamorphic differentiation and to the development of the foliation. The resulting orthogneiss was much weaker that the granodiorite protolith, owing to this reaction and textural softening.

Keywords: foliation development, dissolution–precipitation, reaction softening, textural softening, titanite geochronology, Glastonbury Complex, Connecticut.

SOMMAIRE

Les textures, microstructures, et les schémas de zonation chimique des minéraux d'un orthogneiss granodioritique provenant du complexe de Glastonbury, au Connecticut, mènent à une hypothèse que le développement de la foliation a été facilité par des réactions rétrograde d'hydratation en présence d'une phase fluide aqueuse. Un remplacement partiel des minéraux magmatiques métastables feldspath potassique + hastingsite + magnétite a produit l'assemblage biotite + épidote + quartz, qui définissent la foliation. Ces produits de réaction n'ont pas remplacé les interfaces feldspath potassique – hastingsite; plutôt, c'est soit la biotite ou l'épidote qui a remplacé l'amphibole, et le plagioclase qui a remplacé le feldspath potassique. La biotite et l'épidote se sont formées en couches distinctes qui définissent la foliation de l'orthogneiss au cours de la déformation, tandis que le quartz s'est formé surtout en rubans, contribuant ainsi au développement de la texture. La titanite primaire, riche en terres rares et métastable, est aussi passée en solution, et a été remplacée partiellement par une titanite métamorphique alumineuse et à faible teneur en terres rares. Les teneurs semblables en terres rares de l'épidote et de la titanite montrent que les terres rares issues de la dissolution de la titanite ont contribué localement à la formation de la composante allanite des grains adjacents d'épidote. Le processus au complet était syntectonique, et la plupart des grains font preuve de surcroissances multiples dans la direction de l'extension, telle que définie par les xénolithes étirés. Il y avait une quantité suffisante d'uranium dans les surcroissances de titanite pour permettre une datation par la méthode SHRIMP des coeurs, des zones intermédiaires et des bordures des cristaux. Ces résultats semblent

§ *E-mail address*: wintsch@indiana.edu

indiquer au moins trois événements de croissance rétrograde d'âge alléghanien dans un intervalle d'environ 30 million d'années. Le processus de dissolution – transfert – précipitation décrit non seulement le mécanisme de réaction, mais il a mené aussi à la redistribution des produits de réaction pour former des couches presque monominéraliques, contribuant ainsi à la différenciation métamorphique et au développement de la foliation. L'orthogneiss qui en a résulté est beaucoup plus déformable que le protolithe granodioritique à cause de cette réaction et du ramollissement textural.

(Traduit par la Rédaction)

Mots-clés: développement de la foliation, dissolution–précipitation, ramollissement par réaction, ramollissement textural, géochronologie de la titanite, complexe de Glastonbury, Connecticut.

Introduction

More than 30 years ago, Carmichael (1969) identified an aqueous dissolution – transport – precipitation (DTP) process as the mechanism of reaction in the prograde metamorphism of pelitic rocks. He described several reactions, such as the disappearance of staurolite + muscovite + quartz in favor of garnet + biotite + sillimanite. In this example, the reaction operated *via* a network of locally metasomatic reactions in which the staurolite and muscovite were replaced in their sites, while garnet, biotite, and sillimanite replaced different minerals in different replacement sites. They operated simultaneously with aqueous species communicating among the sites (on the scale of a thin section), such that the net reaction was balanced for all species. However, the individual replacement reactions operated in an open-system metasomatic environment. Carmichael (1969) also discovered that the net reaction involved the local dissolution of plagioclase at one site, and its precipitation in another, in spite of the fact that the participation of plagioclase could not be predicted thermodynamically.

In this paper, we describe textures, mineral compositions, and titanite U–Pb ages that reflect arrested metamorphic reactions in a very different setting from that described by Carmichael (1969). In this example, metastable magmatic minerals in a granodioritic orthogneiss from north-central Connecticut, U.S.A., are incompletely replaced by stable metamorphic minerals. These replacement reactions contrast with those described by Carmichael (1969) in that they are retrograde, they occurred in an originally igneous rock, and the redistribution of reaction products helped to define the metamorphic fabric. We conclude that an aqueous dissolution – transportation – precipitation process like that described by Carmichael (1969) was essential not only to the progress and mechanism of reaction, but also to the development of schistosity in these orthogneisses.

Dissolution – Transport – Precipitation Processes

Carmichael's (1969) dissolution – transport – precipitation mechanism has now been documented not only in other metamorphic environments (*e.g.*, Imon *et al.* 2002) but also in other geological environments. For example, metastable detrital phases dissolve and stable minerals precipitate during diagenesis (*e.g.*, Brown & Ellis 1970, Merino 1975, Milliken 2003). In magmatic crystal–liquid systems, changes in temperature, pressure, and magma composition can cause the resorption of formerly stable minerals and the precipitation of overgrowths of a different composition or of a different phase (*e.g.*, Wones 1979, Pearce & Kolisnik 1990). Pressure solution is another manifestation of this process, in which the solubility of the dissolving phase is increased by strain (*e.g.*, Engelder 1983, Bosworth 1981, Wintsch & Dunning 1985, Bestmann *et al.* 2004), but here the process is a mechanism of deformation. Thus DTP may be a mechanism of both reaction and deformation, but the integration and feedback of these thermally driven (δq) and deformation-driven (δw) processes in syntectonic metamorphic environments have not been widely explored (but see Wintsch & Andrews 1988, Stoeckert *et al*. 1999, Williams *et al.* 2001, Selverstone & Hyatt 2003).

Geological Setting

The rocks under investigation are part of the now-metamorphosed Late Ordovician Glastonbury intrusive complex in northern Connecticut (Leo *et al.* 1984), part of the Bronson Hill arc terrane in central New England. The chemical compositions of the rocks suggest that prior to metamorphism, they were tonalites, granodiorites, and granites (Leo *et al*. 1984). The rocks studied here were granodiorites, as classified by both normative (60–64 wt.% SiO_2) and modal compositions. They contain decimetric inclusions of tonalite, suggesting that the granodiorite and tonalite were comagmatic. The granitic phase (~75 wt.% SiO_2) intrudes the granodiorite (Wintsch *et al*. 1998), but the indistinguishable ages of zircon crystals in the granodiorite and granite (451 ± 5 and 450 ± 2 Ma, respectively: Aleinikoff *et al*. 2002) show that they crystallized simultaneously in the Late Ordovician. However, the ages of magmatic titanite of ~443 and ~425 Ma suggest that anatectic conditions persisted into the Silurian (Aleinikoff *et al*. 2002). This and related volcanic arcs formed offshore of Laurentia, and were accreted to Laurentia during the Devonian Acadian orogeny (Moench & Aleinikoff 2002).

All the rocks of the Glastonbury complex, and in particular the granodioritic gneisses described here, were metamorphosed during the Alleghanian orogeny. Evidence for this comes from the Early Permian U–Pb crystallization ages of metamorphic titanite (Aleinikoff *et al*. 2002), from Early Permian $^{40}Ar/^{39}Ar$ cooling ages of amphibole (Wintsch *et al*. 2003), and from late Pennsylvanian ages of prograde crystallization of titanite and monazite in rocks structurally immediately below the Glastonbury complex (Coleman *et al.* 1997). They were probably also metamorphosed during the Devonian Acadian orogeny, but the absence of Devonian metamorphic titanite in these rocks (Aleinikoff *et al*. 2002) suggests that the grade of Acadian metamorphism here was too low to activate the recrystallization of magmatic titanite. The rocks display variable fabrics, depending on the total strain. Where the strain is low to moderate, as suggested by the aspect ratios of mafic inclusions that are typically >1:10, foliations and lineations are defined by biotite streaks and rods, trails, or ribbons of quartz, plagioclase, and epidote (Fig. 1; Wintsch & Yi 2002).

Results

In this section, we describe textures and fabrics that reveal the process by which the Glastonbury granodiorite was transformed into an orthogneiss. In spite of a metamorphic overprint in the middle amphibolite facies, several magmatic minerals have survived. The most conspicuous mineral is K-feldspar, which occurs as megacrysts. Other magmatic minerals included in these megacrysts are plagioclase, amphibole, biotite and, rarely, magnetite. Some grains of these minerals persist in the matrix, which is dominated by metamorphic minerals, especially plagioclase, biotite, and epidote.

Igneous mineralogy

Megacrysts of K-feldspar up to 2 cm in diameter are the most conspicuous igneous minerals in outcrop and in thin section (Figs. 1, 2), but rarely exceed 20% of the mode. Evidence that these megacrysts are magmatic (see also Vernon 1986) includes: (1) nearly universal Carlsbad twinning (Cb–Tw, Figs. 2A, B), (2) randomly oriented inclusions of albite-twinned plagioclase, magnesiohastingsite, and biotite (Figs. 2, 3C), and (3) their Na-rich bulk composition (~$Or_{82}Ab_{18}$, Wintsch & Yi 2002). Consistent with this is the lack of inclusions of metamorphic minerals, especially the fabric-forming biotite, but also epidote, quartz, and metamorphic titanite. Ubiquitous exsolution-induced lamellae of albite (*e.g.*, Figs. 2B, C) and local grid twinning are inter-

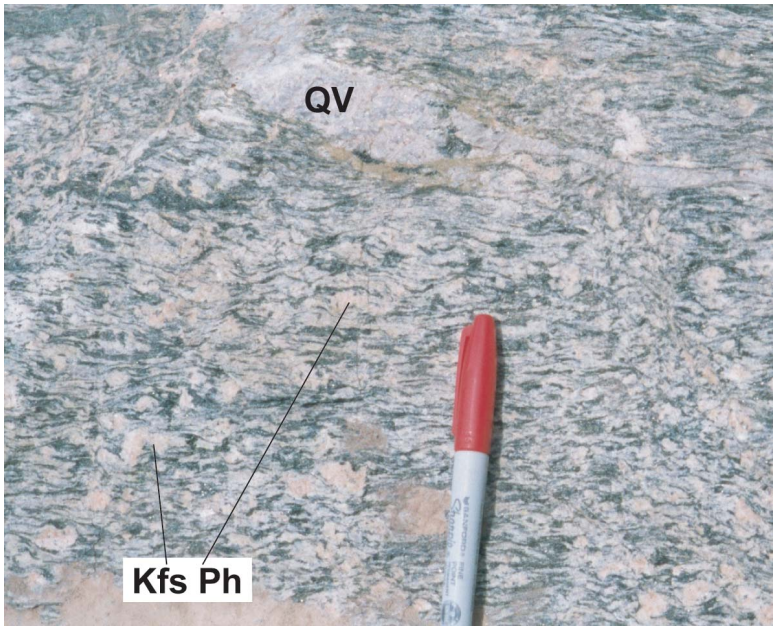

FIG. 1. Outcrop photograph of typical Glastonbury orthogneiss, containing relict phenocrysts of pink K-feldspar (Kfs Ph) now in the shape of σ-porphyroblasts. Aspect ratios of mafic inclusions of ~10:1 suggest moderate strain in this rock. These are surrounded by foliae defined by alternating layers of biotite and epidote, and by quartz ribbons. Pen diameter is 1 cm.

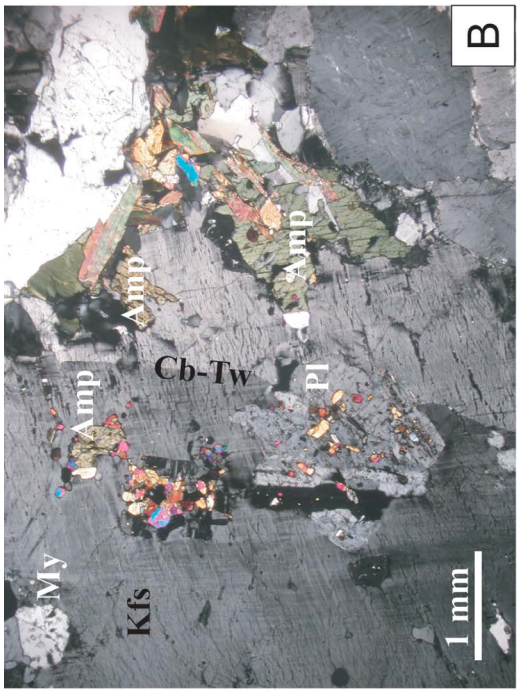
B
My
Kfs
Amp
Amp
Cb-Tw
Amp
Pl
1 mm

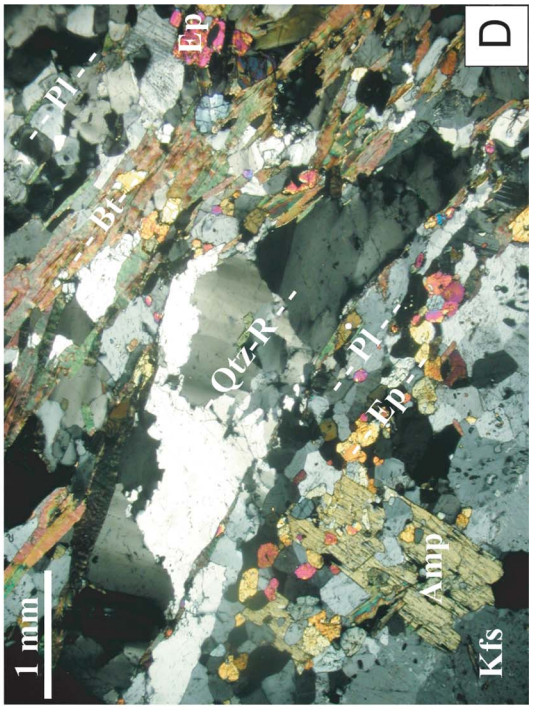
D
Ep
Pl
Bt
Qtz-R
Pl
Ep
Amp
Kfs
1 mm

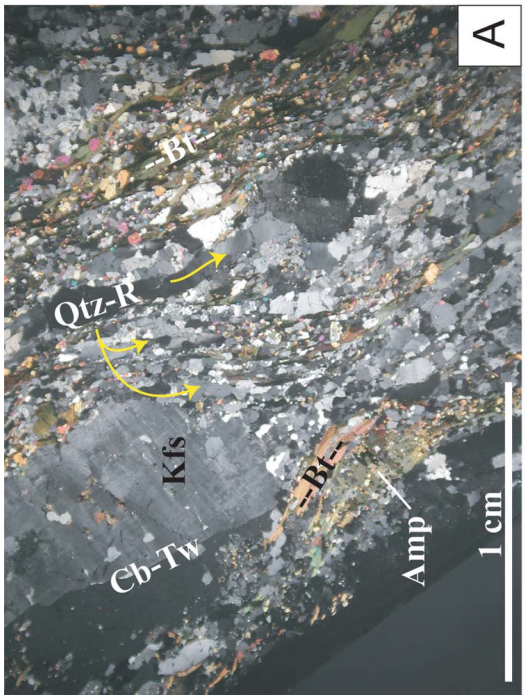
A
Bt
Qtz-R
Kfs
Bt
Cb-Tw
Amp
1 cm

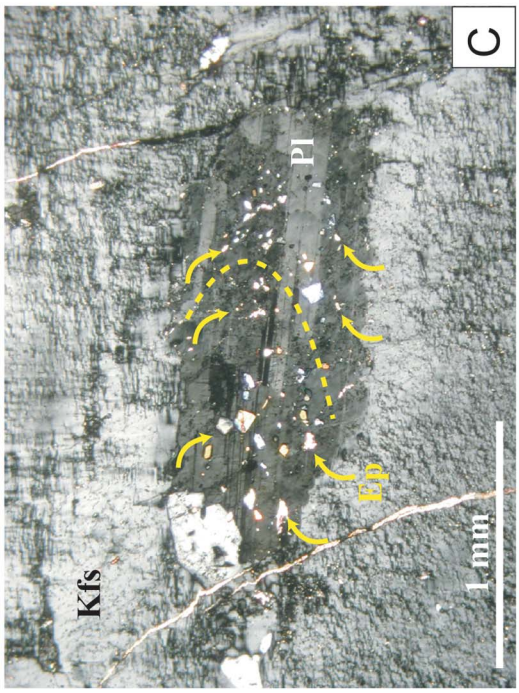
C
Pl
Ep
Kfs
1 mm

preted to have developed during (Alleghanian) metamorphism.

Plagioclase grains interpreted as being magmatic in origin typically display polysynthetic albite twinning but are preserved only within K-feldspar phenocrysts as subhedral to euhedral inclusions (Figs. 2B, C). These contrast with anhedral plagioclase crystals in the matrix that are rarely twinned, and probably metamorphic in origin. Rarely, plagioclase phenocrysts themselves include other subhedral, lath-shaped plagioclase grains. However, all such plagioclase grains are intergrown with epidote (*e.g.*, Figs. 2B, C). Their compositions (~An_{30}) overlap with metamorphic plagioclase grains in the matrix ($An_{20–30}$), and are significantly more sodic than the An_{45} predicted in norm calculations (Leo *et al.* 1984). This suggests that their compositions were modified during metamorphic recrystallization. The small grains of epidote present in most plagioclase grains probably account for the reduced An content of the still twinned magmatic grains. In support of this, some plagioclase laths form trails repeated in a nested arcuate pattern (Fig. 2C), hinting at primary oscillatory chemical zoning established during magmatic crystallization. The inclusion of these twinned and zoned grains within K-feldspar phenocrysts indicates that plagioclase was an early-crystallizing phase, even if its composition has not survived metamorphism.

FIG. 2. Relict magmatic minerals in a metamorphic matrix (crossed polars). A. A relatively large relict Carlsbad-twinned K-feldspar phenocryst (upper left) in a metamorphic matrix of foliae and bands of plagioclase, quartz, and biotite ± epidote. Quartz ribbons occur near the pressure shadow of the phenocryst. Relict magmatic olive green amphibole is indicated. B. Exsolution lamellae of albite in a relict twinned K-feldspar phenocryst that contains inclusions of magmatic amphibole and albite-twinned plagioclase. Myrmekite embays it in the upper left portions of the grain. Inclusions of albite-twinned plagioclase are locally replaced by epidote (red, yellow), but amphibole (green, center-right) is replaced by biotite (brown) only adjacent to the foliated metamorphic matrix. C. Grain of albite-twinned plagioclase included in a grain of magmatic K-feldspar. Small grains of epidote (white, yellow arrows) form trails through the crystal parallel to the yellow dashed line, suggesting the former presence of oscillatory chemical zoning in the plagioclase. D. View of an amphibole crystal (tan) partially included in the margin of a twinned K-feldspar phenocryst (lower left). The amphibole is partially replaced by epidote (yellow, red) and plagioclase (gray) in the upper right and central portions, respectively, where the matrix is well foliated. Replacement is lacking along the K-feldspar – amphibole interface. Metamorphic layering is defined by the quartz ribbon, by plagioclase- and epidote-rich layers below it, and by biotite and plagioclase rich layers above it. Symbols: Amp: amphibole, Bt: biotite, Cb–Tw: Carlsbad twin boundary, Ep: epidote, Kfs: K-feldspar, My: myrmekite, Pl: plagioclase, Qtz–R: quartz ribbon.

Amphibole is a common minor mineral in all samples studied. A magmatic origin for it is indicated by its occurrence as inclusions in some K-feldspar phenocrysts (Figs. 2B, D), and by its uniform chemical composition. All grains analyzed, whether present as inclusions in K-feldspar or in the matrix, have a magnesiohastingsite composition indistinguishable from that described in Wintsch & Yi (2002). This uniform composition independent of local mineral assemblage suggests that all grains have a common origin, and the amphibole inclusions in K-feldspar megacrysts suggest an early-crystallizing magmatic phase.

Both magmatic and metamorphic titanite exist in these rocks. Magmatic titanite is distinguished from metamorphic titanite in that it displays subhedral patterns of zoning, and it contains more ferric iron and rare-earth elements (REE), and less Al, than metamorphic titanite (Table 1, Figs. 4, 5), such that the concentra-

TABLE 1. REPRESENTATIVE RESULTS OF ELECTRON-MICROPROBE ANALYSES OF TITANITE AND EPIDOTE IN ROCKS OF THE GLASTONBURY COMPLEX, CONNECTICUT

	Magmatic titanite		Metamorphic titanite		Epidote			
	high-Ce core	low-Ce core	rim	D.L.	high Ce	medium Ce	low Ce	D.L.
SiO_2 wt.%	30.74	30.98	30.98	(70)	38.07	38.58	38.59	(70)
TiO_2	36.07	36.46	36.29	(150)	0.05	0.08	0.10	(140)
P_2O_5	0.06	0.07	b.d.t.	(190)	b.d.t.	b.d.t.	b.d.t.	(180)
Nb_2O_5	0.10	n.d.	0.68	(310)	0.07	n.d.	b.d.t.	(280)
Al_2O_3	1.23	1.17	1.68	(60)	24.23	24.60	24.81	(60)
Fe_2O_3	1.63	1.51	0.86	(210)	12.20	12.33	12.22	(190)
Y_2O_3	0.23	0.08	0.12	(280)	0.12	0.06	n.d.	(260)
La_2O_3	0.13	0.13	n.d.	(520)	0.10	n.d.	n.d.	(490)
Ce_2O_3	0.61	0.38	0.07	(430)	0.56	0.16	0.05	(380)
Pr_2O_3	0.20	0.10	0.12	(640)	0.08	0.08	0.08	(630)
Nd_2O_3	0.29	0.14	n.d.	(380)	0.35	0.17	n.d.	(340)
Sm_2O_3	0.15	0.07	n.d.	(650)	0.08	n.d.	b.d.t.	(650)
MnO	0.15	0.12	0.12	(160)	0.30	0.33	0.35	(150)
CaO	27.66	28.08	28.49	(100)	22.31	23.00	23.16	(90)
F	0.31	0.38	0.29	(350)	b.d.t.	n.d.	n.d.	(360)
O=F	-0.13	-0.16	-0.12		n.c.	n.c.	n.c.	
Total	99.43	99.50	99.57		98.52	99.39	99.34	
Si *apfu*	1.013	1.014	1.011		6.022	6.027	6.019	
Ti	0.894	0.898	0.891		0.007	0.010	0.011	
P	0.002	0.002	-		-	-	-	
Nb	0.002	-	0.010		0.005	-	-	
Al	0.048	0.045	0.065		4.517	4.530	4.561	
Fe	0.040	0.037	0.021		1.453	1.449	1.435	
Y	0.004	0.001	0.002		0.010	0.005	-	
La	0.002	0.002	-		0.006	-	-	
Ce	0.007	0.005	0.001		0.033	0.009	0.003	
Pr	0.002	0.001	0.001		0.005	0.005	0.005	
Nd	0.003	0.002	-		0.020	0.010	-	
Sm	0.002	0.001	-		0.005	-	-	
Mn	0.004	0.003	0.003		0.040	0.044	0.046	
Ca	0.977	0.985	0.996		3.781	3.850	3.871	
F	0.032	0.039	0.030		-	-	-	
Total	3.032	3.035	3.031		15.901	15.937	15.948	

Operating conditions: 15 kV, 40 nA. The elements K, Na, Ti, Mg, Zr, Sn, W, Ta, Yb, Dy, Er were sought. All are lower than the detection limit, D.L., expressed in ppm; n.d.: not detected, n.c.: not calculated, b.d.t.: below detection threshold. The formulae are calculated on the basis of five atoms of oxygen for titanite and 25 for epidote, using the valence of the oxide component listed.

tions of Fe^{3+} and Al are nearly equal (Fig. 6). Its magmatic origin is confirmed by its Late Ordovician age [443 ± 6 Ma (2σ): Aleinikoff *et al*. (2002)], which overlaps with the age of magmatic zircon from the same sample [451 ± 5 Ma (2σ)]. Oscillatory and sector-zoning that is conspicuous in back-scattered electron imaging (Aleinikoff *et al*. 2002) and element mapping of these grains are caused by oscillating concentrations of Al, Fe^{3+}, and the REE (Fig. 4, Table 1). Ferric iron and Al, together with Nb, substitute for Ti in the structure (Fig. 5). The decrease in charge caused by this substitution is balanced by REE substitution for Ca, such that Ti + Ca = Fe^{3+} + Al + REE. The lack of correlation of F^{1-} with Al^{3+} ions (Fig. 6) indicates that the substitution of F^{1-} + Al^{3+} for Ti^{4+} + O^{2-} is not important. Magmatic grains of titanite are rarely in contact with any other minerals in the rock. On the contrary, they are universally isolated from the surrounding metamorphic assemblage by a rim and overgrowth of metamorphic titanite (*e.g.*, Fig. 4.).

Several other minerals were probably also magmatic. Biotite that occurs as inclusions in K-feldspar megacrysts was almost certainly magmatic, even though its composition is only slightly richer in Fe and ^{VI}Al than fabric-forming metamorphic biotite in the matrix. These inclusions occur as laths up to 500 μm long, and as equant grains up to ~250 μm in diameter. They are always in random orientation. Magnetite also occurs

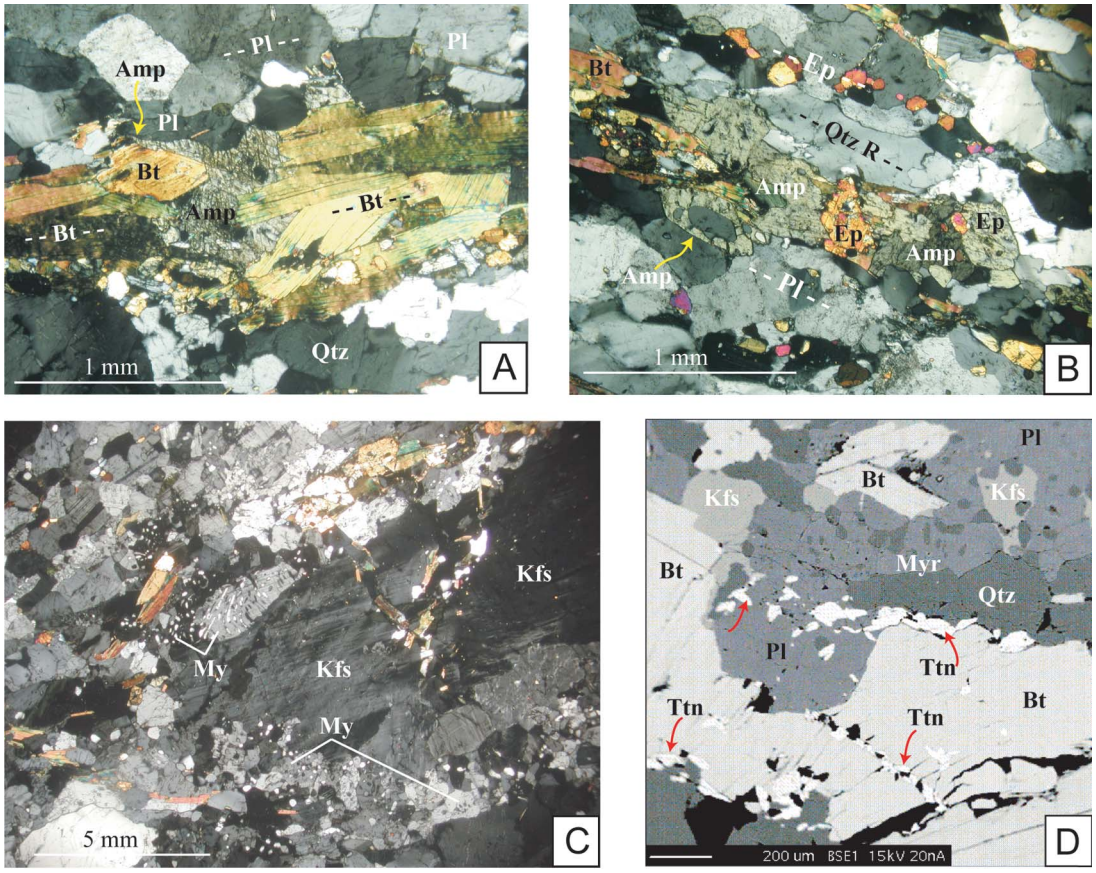

FIG. 3. Textures reflecting arrested metamorphic replacement relationships and magmatic inclusions. A. A hastingsite grain partially replaced by biotite in a biotite-rich foliation plane. Plagioclase also embays the amphibole along the upper left boundary, leaving only a narrow finger of amphibole (yellow arrow) separating biotite from plagioclase. Foliae of biotite and plagioclase are indicated with the dashed lines. B. A large grain of hastingsite (pale green) partially replaced by epidote (orange, green). Foliae of epidote, quartz and plagioclase are indicated with the dashed lines. C. Randomly oriented flakes of biotite in a magmatic K-feldspar crystal embayed by myrmekitic intergrowths of quartz and plagioclase. D. A back-scattered electron image showing titanite grains (white) intergrown with biotite (pale gray) and plagioclase (dark gray) in a matrix of K-feldspar (medium gray) and quartz (darkest gray). Symbols as in Figure 2.

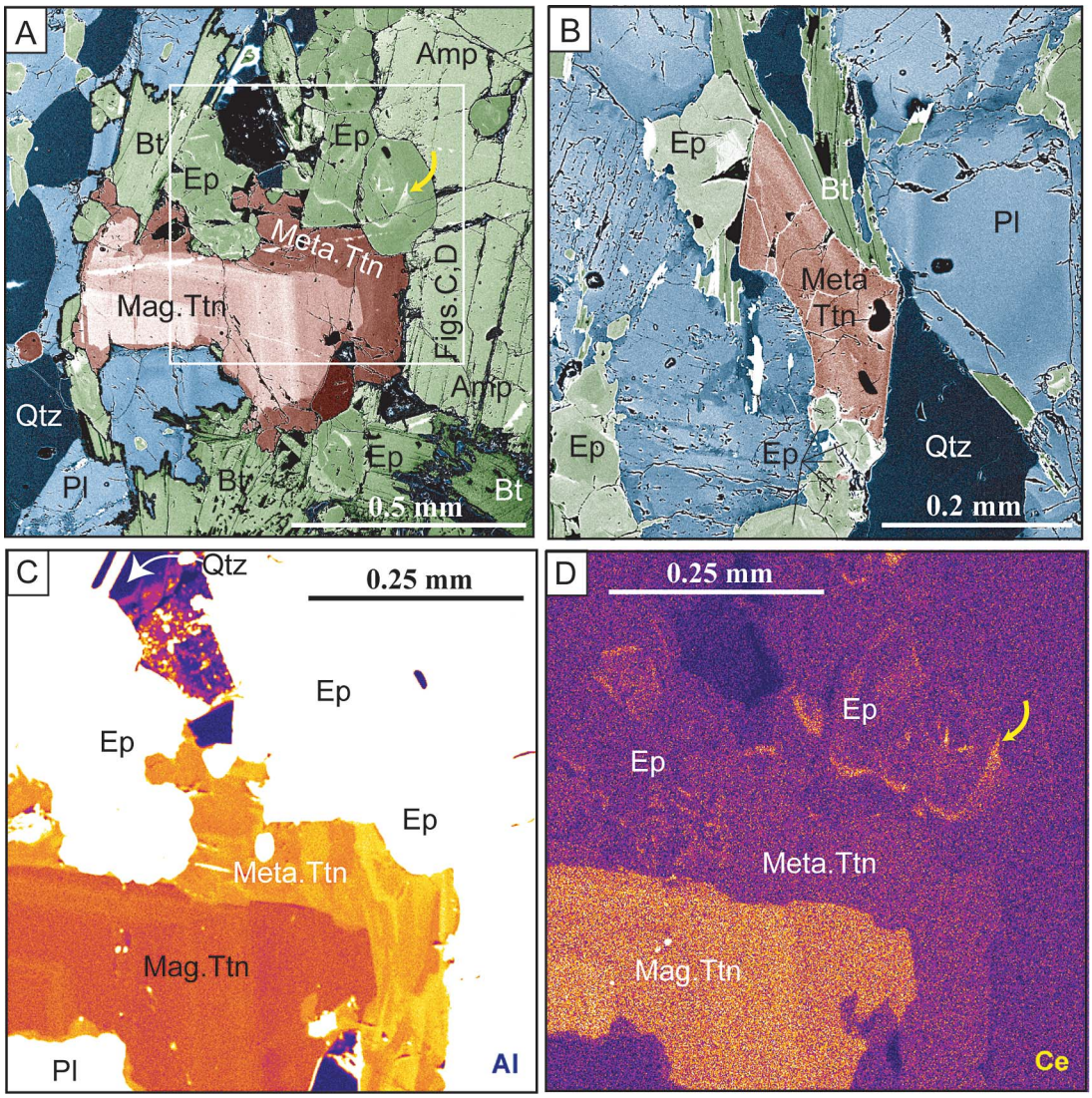

FIG. 4. Colorized back-scattered electron images and element maps of magmatic and metamorphic titanite. A. An anhedral grain of magmatic titanite with oscillatory zoning (brighter shades of tan indicate higher REE contents) completely isolated from the matrix by an overgrowth of metamorphic titanite (brown) intergrown with epidote. These zoned grains of epidote (dark green) contain allanite-rich bands (white, yellow arrows) that define cores, mantles, and rims. Splinter-like biotite is medium green, amphibole is pale green, plagioclase is blue, with darker shades richer in the albite end-member, and quartz is indigo to black. White box indicates areas of Figures 4C and 4D. B. A subhedral zoned grain of metamorphic titanite, with darker shades of brown richer in Al, intergrown with epidote at the base. Other colors as in Figure 4A. C. An element-distribution map in which brighter colors indicate higher concentrations of Al. The map shows euhedral zoning in magmatic titanite, and fluctuating zoning in the metamorphic overgrowth. Epidote grains are white. D. An element-distribution map in which brighter colors indicate higher concentrations of Ce. The map confirms that the magmatic core of titanite is REE-rich, and that the white bands in epidote (Fig. 4A) are also relatively rich in REE (yellow arrow).

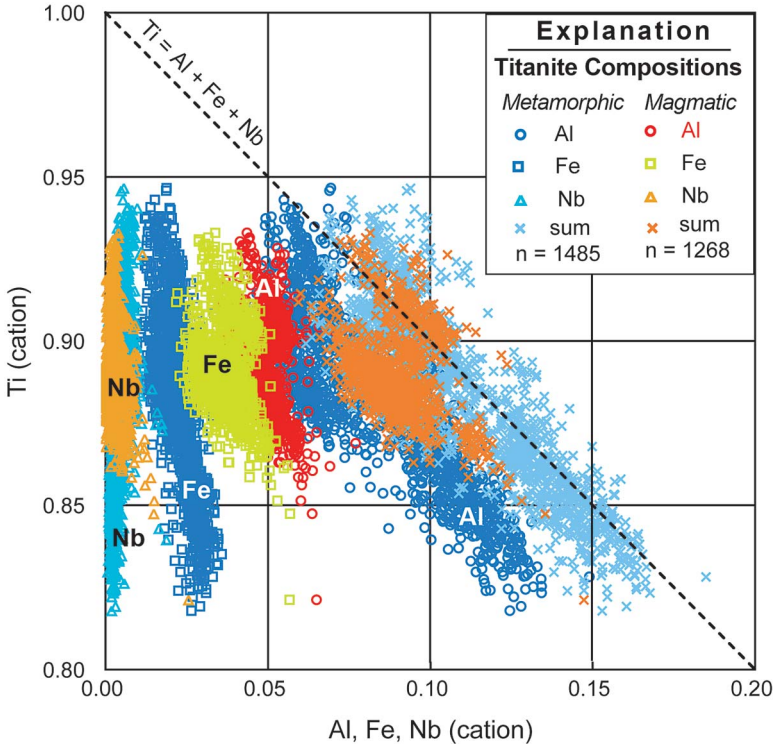

FIG. 5. The variation of Al, Fe^{3+}, and Nb cations with Ti, calculated on the basis of five atoms of oxygen. Metamorphic titanite (symbols in shades of blue) contains less Fe and more Al than magmatic titanite. The strong negative correlation of Al + Fe + Nb with Ti, and the sum of Al + Fe + Nb + Ti ≈ 1, indicate the substitution Ti = Al + Fe + Nb (dashed line) in all titanite.

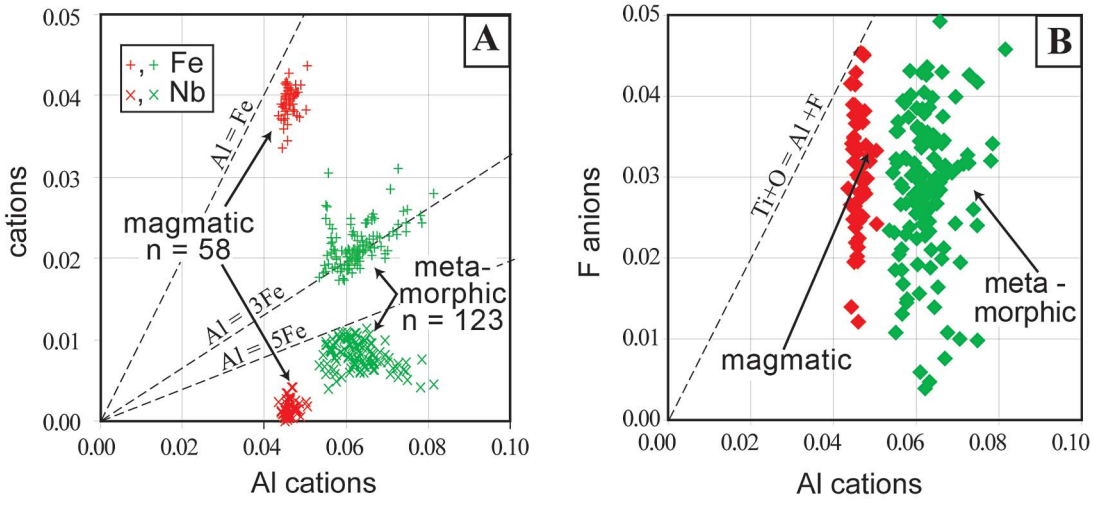

FIG. 6. A comparison of a subset of the compositions of titanite of magmatic and metamorphic origin from Figure 5. A. A diagram showing that metamorphic titanite contains three times the Al/Fe and twice the concentration of Nb. B. The independence of F anion and Al cation concentrations shows that the Al + F exchange for Ti + O is not an important exchange in these grains.

rarely as subhedral inclusions in K-feldspar megacrysts. Although it does not occur in the present metamorphic matrix, its former existence as a viable magmatic accessory mineral is likely. Quartz was undoubtedly an interstitial magmatic phase in these intermediate rocks, but the thorough recrystallization of the matrix, including quartz, and the lack of quartz inclusions in K-feldspar, make this impossible to prove.

Metamorphic mineralogy

The most conspicuous aspect of the metamorphic assemblage in the granodioritic orthogneiss described here is the preferred orientation and distribution of plagioclase, epidote, quartz, and especially biotite, that together define strong foliations (Figs. 2A, D, 3A). It commonly wraps around K-feldspar phenocrysts to produce augen (Figs. 1, 2A) which may show a σ-type geometry in an S–C fabric (Wintsch & Yi 2002) with the sense of shear indicating top to the south-southeast (Wintsch *et al*. 2003). This fabric also includes a penetrative mineral lineation defined by quartz rods, and plagioclase-, biotite-, and epidote-rich streaks that in cross section appear as mono- or bimineralic bands (Figs. 2A, D, 3A, and 7A, C).

Untwinned plagioclase is the most abundant metamorphic mineral. It occurs in discontinuous bands and layers up to 1 mm thick and 10 mm long (Figs. 2A, D, 3B, 7C). Most grains show repeated zones with compositions ranging from An_{30} to An_{20}: larger grains show three or more chemical oscillations (Wintsch & Yi 2002). Another common occurrence of plagioclase is in lobate myrmekitic structures embaying magmatic K-feldspar augen (Fig. 3C).

Biotite is the most conspicuous metamorphic mineral, defining foliations and lineations in both outcrop and thin section. Flakes are typically several tenths of a millimeter long, but may be >1 mm in length (Figs. 2A, B, 3A, and 7). Bands of grains one to five flakes thick anastomose around K-feldspar phenocrysts (Fig. 2A), forming foliae 2 to 30 mm long. These grains are commonly intergrown with epidote, amphibole, and metamorphic titanite (Figs. 2, 3D, and 7).

Epidote commonly occurs as equant grains 50–300 μm in diameter in bands intergrown with biotite or titanite (Figs. 4, 8A), or in bands of almost pure epidote (Figs. 2D, 3B, 7). These grains vary in composition, $100Fe^{3+}/(Al + Fe^{3+})$ from 22 to 26, as found by Wintsch & Yi (2002). Epidote also occurs as isolated grains 10–100 μm in diameter within twinned plagioclase grains (Figs. 2B, C). These grains contain less Fe than matrix epidote, and are typically weakly zoned, with $100Fe^{3+}/(Al + Fe^{3+})$ contents increasing from 18 to 22 from core to rim. Many grains contain thin bands in which rare-earth elements exceed 1.3 wt.%, and several thousand times chondrite (Table 1, Fig. 9). These bands define ovoid, lobate and, less commonly, subhedral patterns (Figs. 4A, D; Wintsch & Yi 2002).

Most quartz grains occur in two structures: (1) as ribbons up to 5 mm wide and 2 cm long between biotite foliae (Figs. 2A, D, 3B, and 5C), and (2) in pressure shadows "behind" K-feldspar phenocrysts (Fig. 2A). Locally, these ribbons are large enough to produce veins (Fig. 1). However, quartz also occurs as isolated 200 μm grains in the matrix associated with plagioclase and as small vermicular grains in myrmekite (Figs. 2B, 3C).

K-feldspar is a minor metamorphic mineral in the matrix. It is typically associated with plagioclase in plagioclase-rich lamellae, where it may form in extension sites, and also forms rinds around quartz grains, isolating them from enclosing plagioclase (Fig. 7B).

Metamorphic titanite occurs as an overgrowth and as crack fillings on magmatic cores (Aleinikoff *et al*. 2002) and as isolated subhedral grains associated with fabric-forming biotite (Figs. 3D, 4B). Evidence that some titanite crystallized during metamorphism comes from its intergrowth with metamorphic epidote and fabric-forming biotite, from the truncation of oscillatory zoning patterns of overgrown magmatic cores, and from the subhedral outlines of isolated grains and internal patterns of zoning (Figs. 4, 8). Metamorphic titanite also is distinctive chemically in that it contains higher concentrations of Al and generally higher Nb but lower Fe^{3+}, Y, Ce and other REE (Table 1, Figs. 5, 6, and 8) and ten times lower U and Th/U (Aleinikoff *et al.* 2002).

Metamorphic titanite is universally zoned. The zoning is weakly visible in BSE imaging (Figs. 4A, 4B, 8; Aleinikoff *et al.* 2002), but becomes quite conspicuous with element mapping (Fig. 4C), where the fluctuating concentrations may define complicated patterns. The zoning pattern is quantified by electron-microprobe analyses in Figure 8 (Wintsch & Yi 2002). For example, patterns defined by fluctuations in composition show cyclic rises in Al and Fe toward the rims, which typically define three stages of overgrowth, identified as core, mantle, and rim (Fig. 8).

Confirmation of the metamorphic origin of this titanite comes from the SHRIMP analyses reported by Aleinikoff *et al*. (2002), which show that these grains crystallized at 265 ± 8 Ma (2σ), ~180 m.y. after the magmatic cores. These ages were calculated from data collected from all three zones of growth during three analytical sessions. Unfortunately, the low uranium concentrations and young ages resulted in large analytical uncertainties that precluded using the ages themselves to identify and discriminate these multiple events of growth. The Tera–Wasserburg diagram (Fig. 10) shows the overlap of the analytical data. Subsequent to this isotopic work, we analyzed each titanite grain by electron microprobe (*e.g.*, Fig. 8) to determine the particular growth-zone from which each isotopic analysis of Aleinikoff *et al*. (2002) was obtained. The results of this analytical campaign (Fig. 5) identified the zones shown in Table 2. Weighted averages of $^{206}Pb/^{238}U$ ages, subdivided into chemically distinguished groups of core, mantle, and rim, yield ages of 291 ± 8, 268 ± 8, and 259

± 10 Ma, respectively (Table 2; see insets, Fig. 10), in agreement with ages calculated by regressing the isotopic data that are uncorrected for common Pb, as shown in the Tera–Wasserburg diagram (Fig. 10). These ages are progressively younger from core to rim, as required by the "stratigraphic" sequence of overgrowths, but the errors in the ages are large enough to allow overlap in the times of crystallization of mantle and rim. The data nevertheless suggest that 30 m.y. elapsed between the crystallization of the core and rim of these grains.

Discussion

Two contrasting assemblages of minerals are present in these orthogneisses. One is a relict igneous assemblage, containing K-feldspar phenocrysts, hastingsite,

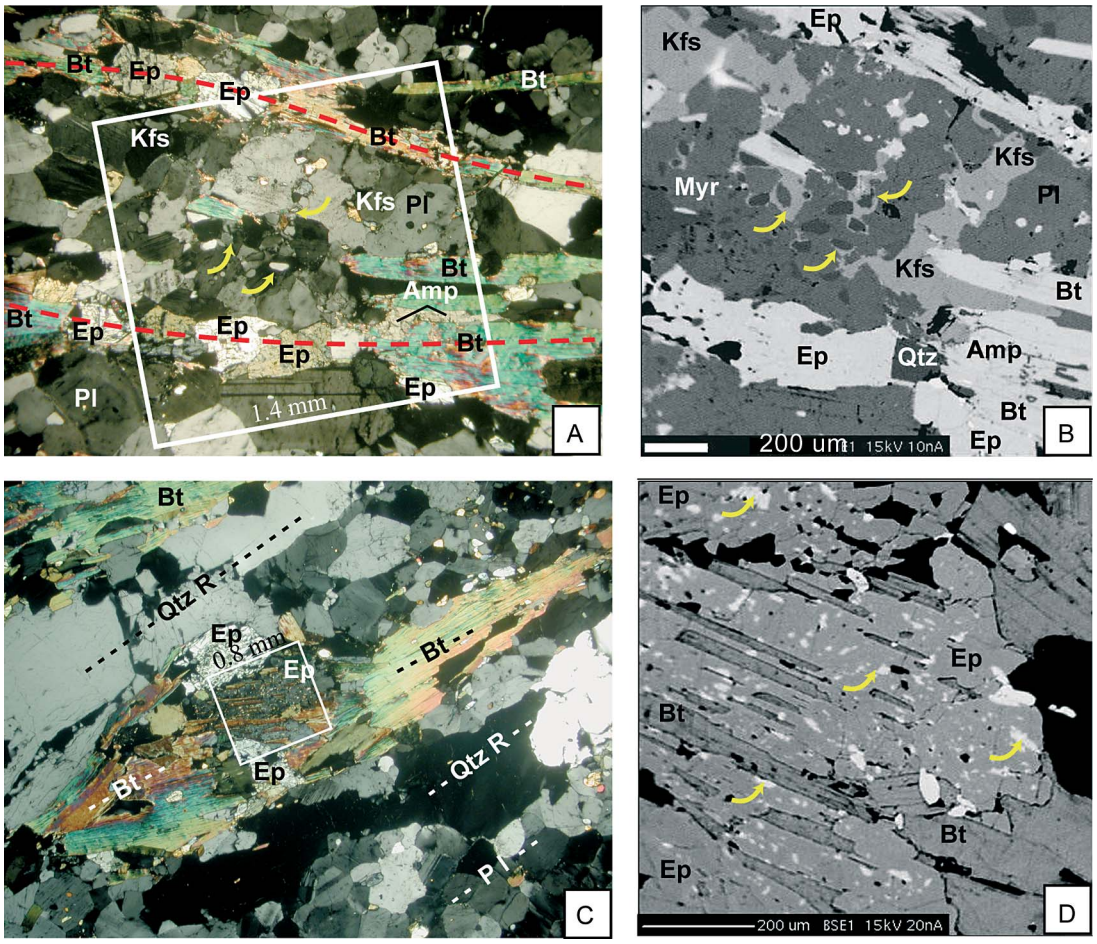

Fig. 7. Micrographs of textures reflecting the arrested replacement of biotite by epidote (reaction 6, Table 4). A. A view of foliae (dashed red lines) defined by blue and green flakes of biotite that are partially replaced by epidote (white and pastel grains) in a matrix of quartz and plagioclase. A blade of pale tan amphibole (SE quadrant) is largely replaced by sandwiching biotite flakes. Rinds of K-feldspar (yellow arrows) partially replace quartz. Location of Figure 7B is indicated by the 1.4 mm white box. Crossed polars. B. A back-scattered electron image of the region outlined in Figure 7A. Fe-rich grains of biotite, epidote, and amphibole all are very pale gray, K-feldspar is medium gray, plagioclase is darker gray, and quartz is the darkest gray. The image shows tentacles of K-feldspar selectively replacing quartz vermicules in a myrmekitic intergrowth, using K^+ released in the epidote replacement of biotite (see text). C. View of a biotite-rich layer (orange and blue flakes; dashed red lines) between two quartz ribbons. Epidote (gray and white, high-relief grains) interrupt this layer and include parallel flakes of orange biotite (white box, 0.8 mm sides). Crossed polars. D. A back-scattered electron image of the region in the white box of Figure 7C showing biotite inclusions (dark gray laths) in epidote (medium gray) host. Small white grains of titanite (*e.g.,* yellow arrows) included in epidote are interpreted to be by-products of the replacement of biotite by epidote (see text).

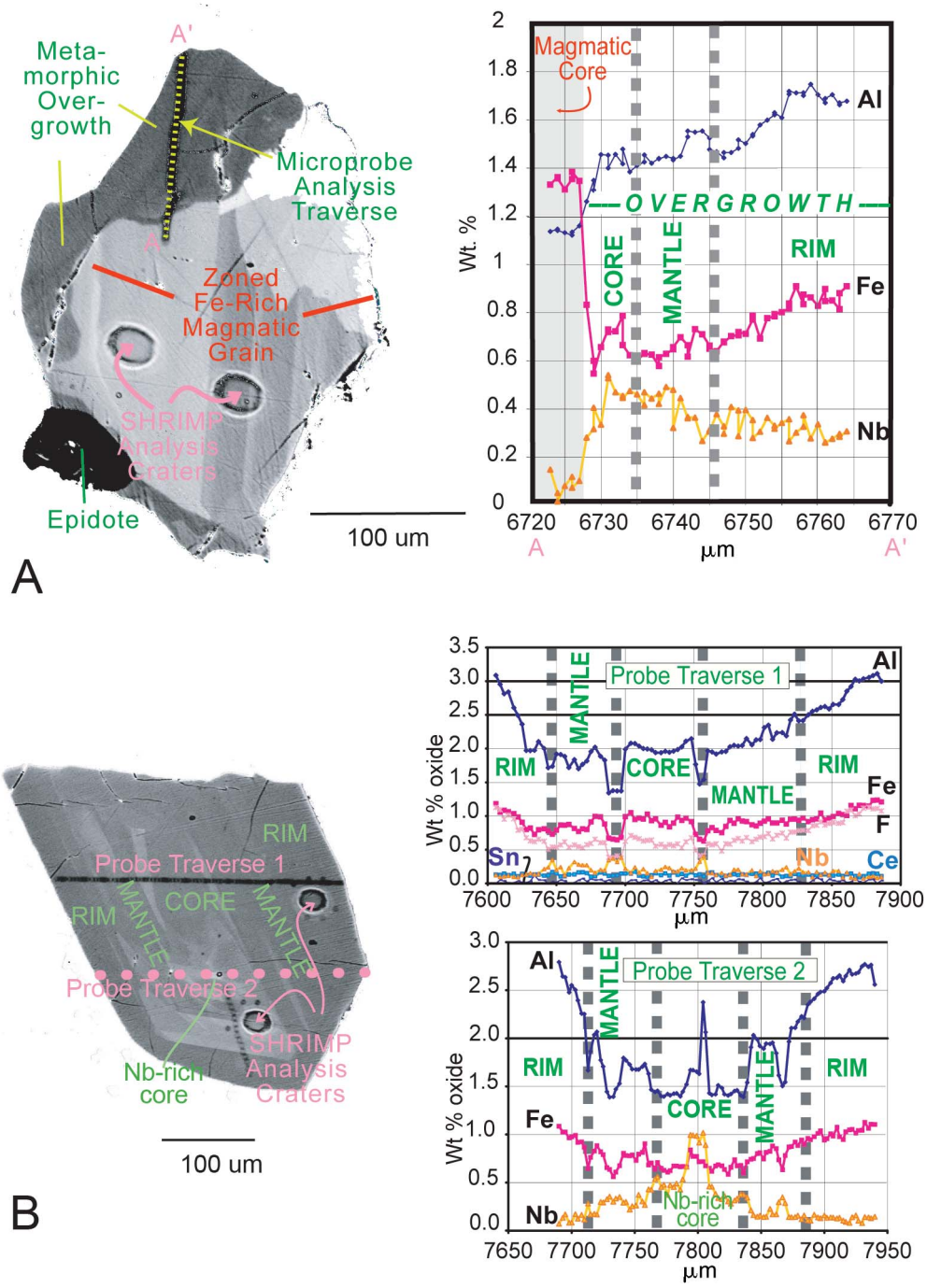

FIG. 8. Back-scattered electron images showing the positions of electron-microprobe traverses across composite grains of titanite. A. A compound rim of metamorphic titanite (intergrown with epidote) overgrown on a partially replaced and complexly zoned magmatic core. B. A subhedral grain of metamorphic titanite showing multiple overgrowths on a metamorphic core. Pale gray regions reflect relatively high concentrations of Nb. The zoning profiles, with increasing concentrations of Al from core to mantle to rim, are shown in the adjacent graphs.

plagioclase, titanite, quartz (?), biotite, and magnetite, the latter two preserved only as inclusions in the phenocrysts. The second is an overprinting metamorphic assemblage, including newly crystallized K-feldspar, plagioclase, titanite, epidote, biotite, and quartz. In this section, we identify the processes that led to the destruction of the former igneous assemblage and its replacement by the overprinting metamorphic assemblage.

Replacement of the metastable igneous assemblage: hastingsite + K-feldspar

The igneous assemblage reconstructed above, especially hastingsite + K-feldspar (~Or_{80}) + magnetite, became metastable in the hydrous metamorphic environment of the epidote amphibolite facies, whereas plagioclase and quartz persisted in both environments. A reaction relationship developed among the reactants (amphibole + K-feldspar + magnetite) and products (biotite + epidote) such that amphibole + K-feldspar + magnetite reacted to give biotite + epidote. This relationship is shown schematically in Figure 11 where the epidote–biotite tie-line pierces the metastable three-phase K-feldspar – amphibole – magnetite shaded tie-plane close to the K-feldspar – amphibole edge of the region. This relationship indicates that magnetite was a minor reactant. In fact, magnetite is no longer present in the matrix, apparently being completely consumed by the progress of the reaction. In fact, the reaction is continuous, given the solid solution in several phases, and the merger of components in Figure 11. Nevertheless, a degenerate reaction of amphibole + K-feldspar = biotite + epidote can be balanced without magnetite using simplified results of the electron-microprobe analyses given in Table 3 (reaction 1, Table 4):

$$56\ \text{Kfs} + 52\ \text{Amp} + 30\ H_2O + 7\ O_2 = 56\ \text{Bt} + 52\ \text{Ep} + 196\ \text{Qtz}.$$

Where the fluid did not have access to the Kfs + Amp pair, as was apparently the case within K-feldspar phenocrysts, the reaction did not occur. For example, the lower-left margins of the amphibole grains in Figures 2B and 2D are enclosed in K-feldspar phenocrysts, and appear unreacted. However, matrix amphibole is commonly partially replaced by biotite (Figs. 2B, 3A) or epidote (Figs. 2D, 3B).

The intergrowth of Or – Amp – Bt – Ep – Qtz in the replacement relationship predicted by reaction 1 (Table 4) is not found in thin section. On the contrary, amphibole is generally intergrown with only one or two minerals, commonly including biotite or epidote (Figs. 2, 3). Figure 3A shows a typical grain of amphibole strongly embayed by biotite from the left and right, whereas plagioclase has embayed the grain from above, leaving only a narrow finger of amphibole in the upper left (yellow arrow). The possibility that amphibole has replaced biotite can be ruled out because amphibole grains are anhedral, and completely unzoned, contrary to expectations had they crystallized during a prograde metamorphic event. On the contrary, the amphibole composition is uniform from grain to grain and sample to sample, supporting the interpretation that all grains crystallized together from a single magma (see Wintsch & Yi 2002). Such a replacement reaction is locally metasomatic and must be written as: amp + aqueous ions = bt + qtz + aqueous ions, reflecting the locally open, metasomatic system (Table 2, reaction 2).

Amphibole is commonly intergrown with epidote, and replaced by epidote as well. The epidote may occur as small anhedral grains (*e.g.*, Fig. 2D) or as larger subhedral grains (Fig. 4A), such as those shown in Figure 3B, where epidote embays and truncates an optically continuous amphibole. Thus it is much more likely that epidote has replaced amphibole rather than the reverse reaction. This reaction is also locally metasomatic, requiring the introduction of aqueous ions, and releasing SiO_2 as shown by reaction 3 (Table 4).

Whereas epidote replaces amphibole in some sites, it commonly replaces plagioclase in others. The subhedral shape of grains that truncate zoning in adja-

TABLE 2. SHRIMP $^{206}Pb/^{238}U$ AGES FOR METAMORPHIC TITANITE FROM GRANODIORITE GNEISS, GLASTONBURY COMPLEX, CONNECTICUT*

sample[1,2]	location: zoning[3]	$^{206}Pb/^{238}U$ age (Ma)	error[4] (Ma)
	Core		
1cl-4.1	c:lg	298.8	9.5
1cl-5.1	c:lg	312.8	60.5
1cl-7.1	c:lg	299.5	6.7
2br-16.1	r:b	268.6	13.8
2br-16.6	r:b	338.5	63.9
2br-10.3	r:b	277.1	8.2
2br-8.3	r:b	296.1	43.5
3cl-25.1	c:g (pg)	280.8	34.1
3cl-12.1	c:w	310.4	17.8
3cl-35.1	c:g (pg)	284.2	15.2
weighted average of the $^{206}Pb/^{238}U$ ages: 291 ± 8 Ma			
	Mantle		
1cl-1.1	c:lg	265	115.2
1cl-6.1	c:lg	289.4	9.3
3cl-66.1	c:w	203.4	33.7
3cl-22.1	c:g (pg)	268.5	7.9
3cl-22.2	c:w (pg)	250.6	8.0
3cl-22.3	c:w (pg)	268.6	8.3
3cl-12.2	c:g	273	13.2
3cl-51.1	c:g (pg)	278.3	8.4
3cl-55.1	c:w	272.7	7.2
3cl-55.2	c:g	259	7.2
3br-34.3	r:b	281.2	45.7
weighted average of the $^{206}Pb/^{238}U$ ages: 268 ± 9 Ma			
	Rim		
2br-27.5	r:b	265.3	7.6
3cl-66.2	r:g	249	10.2
3cl-64.2	r:w (pg)	258.6	9.4
3cl-5.3	r:g	234.5	103.0
weighted average of the $^{206}Pb/^{238}U$ ages: 259 ± 10 Ma			

Notes: 1 The first number refers to the analytical session (from Aleinikoff *et al.* 2002). Abbr.: br (brown grain), cl (clear grain). 2 The groupings into core, mantle, and rim are determined by patterns of chemical zoning (Fig. 8). 3 Abbreviations: c (core), r (rim), lg (light gray in BSE), w (white in BSE, no zoning), g (gray in BSE), b (black in BSE), pg (pale green in color). 4 1σ errors.

cent plagioclase grains is consistent with this interpretation (Wintsch & Yi 2002). Moreover, concentric patterns of small grains within igneous plagioclase probably reflect selective replacement of calcic zones in this magmatic crystal (Fig. 2C). Finally, the ferric iron content of epidote within plagioclase is lower than that in the matrix, consistent with a plagioclase reactant. Nevertheless, epidote replacement of plagioclase requires the introduction of Ca and Fe, and the export of Na and SiO_2 (Table 4, reaction 4).

Net reaction 1 predicts the replacement of K-feldspar phenocrysts, yet biotite and epidote are never seen intergrown with K-feldspar in a replacement-like relationship. On the contrary, plagioclase in myrmekitic structures commonly replaces the K-feldspar megacrysts at their margins (Fig. 2A). Quartz is a reaction product, and apparently coprecipitates with the replacing plagioclase in its typical vermicular intergrowth (*e.g.,* Simpson & Wintsch 1989). A reaction balanced for a typical anorthite content of 25% is given in Table 4 (reaction 5).

A metasomatic "Carmichael loop"

The four replacement reactions described above are all locally metasomatic, both importing and exporting alkalis, Fe^{2+} and Mg^{2+}, H^+, and SiO_2. However, when added together, the aqueous ionic species are inferred to communicate among the four reactions sites such that the ionic species cancel, and the net reaction (reaction 1, Table 4) is closed to cations on the scale of cm or dm. SiO_2 is an exception to this rule. Examination of the textures (Figs. 2–4, 7) supporting the individual metasomatic reactions shows that the SiO_2 evolved in each of them does not precipitate locally at the replacement site. Instead, quartz is concentrated in pressure shadows or as ribbons between biotite + epidote foliae (Figs. 2A, D, 3B, and 7C). These relationships are shown in Figure 12, where cations are transported (through a grain-boundary fluid) among the reaction sites, but quartz precipitates independently as a ribbon.

This process of dissolution, transport, and precipitation (DTP) is identical to the mechanism that Carmichael (1969) identified for prograde metamorphic reactions in pelitic rocks. However, our results indicate that this mechanism of metasomatic reactions operating simultaneously, and communicating chemically in a "Carmichael loop" among several reaction sites, is not restricted to pelitic rocks. On the contrary, DTP also facilitates these reactions in orthogneisses undergoing hydration. The introduction of H_2O is confirmed by the operation of reaction 1 (Table 4) to the right, and the presence of H_2O probably enhanced chemical communication among replacement sites.

Metasomatic replacement of biotite

A second example of metasomatic replacement is also present in these rocks: the replacement of biotite by epidote. Most biotite occurs as flakes in foliae, and many of these are intergrown with epidote. Less commonly, epidote completely interrupts the biotite foliae, suggesting biotite replacement by epidote. For example, epidote has completely replaced laths of biotite in two adjacent foliae (dashed red curves, Fig. 7A). Some of the most compelling evidence that this is a replacement texture comes from the incomplete replacement of biotite by epidote (Fig. 7C), where epidote contains inclusions of optically continuous biotite. Back-scattered electron petrography (Fig. 7D) shows that no matrix plagioclase or quartz is present along the boundaries, but bright titanite grains (yellow arrows) included within the epidote are obvious. Such inclusions are not surprising given that biotite contains over 2.0 wt.% TiO_2 (Wintsch & Yi 2002) that cannot be taken up in epidote solid-solution (Table 1). This association of titanite with biotite and epidote thus provides strong support for the replacement of biotite by epidote, where titanite is a reaction by-product.

TABLE 3. COMPOSITIONS[1] AND MOLAR VOLUMES OF MINERALS AS USED TO BALANCE REACTION IN TEXT

Mineral	Formula	ΔV (cm³)	ref.
Amphibole	$Ca_2[(Mg,Fe)_{3.5}Fe^{3+}_{0.46}Al_{1.04}][Si_{6.5}Al_{1.5}]O_{22}(OH)_2$	278.	2
K-feldspar	$KAlSi_3O_8$	108.	3
Plagioclase	$Na_{0.75}Ca_{0.25}Al_{1.25}Si_{2.75}O_8$ and $CaAl_2Si_2O_8$	100.	3
Biotite	$K[(Mg,Fe)_{2.75}Al_{0.25}][Si_{2.75}Al_{1.25}]O_{10}(OH)_2$	150.	3
Epidote	$Ca_2FeAl_2Si_3O_{12}(OH)$	138.	3
Quartz	SiO_2	22.69	3
Titanite	$CaAlSiO_4(OH)$ [Al–OH component]	55.75	3

[1] Simplified compositions based on results of electron-microprobe analyses in Wintsch & Yi (2002).
[2] Interpolated from data compiled in Dahl (1996).
[3] from Smyth & Bish (1988).

TABLE 4. SUMMARY OF BALANCED REACTIONS[1] IDENTIFIED IN THE TEXT

No.	Reaction	ΔV_r[2]	ΔV_r[3]
1	52 Amp + 56 Or + 30 H_2O + 7 O_2 = 56 Bt + 52 Ep + 196 Qtz	−2.3	
2	33 Amp + 56 K^+ + 38.5(Fe^{2+}, Mg^{2+}) + 46 H^+ = 56 Bt + 66 Ca^{2+} + 15 Fe^{3+} + 61 SiO_2	+7	−8
3	19 Amp + 15 Fe^{3+} + 66 H^+ + 10 Ca^{2+} = 24 Ep + 66.5 (Fe^{2+}, Mg^{2+}) + 40 H_2O + 51 SiO_2	+21	−37
4	44.8 $Pl(An_{25})$ + 4.5 Ca^{2+} + 28(Fe^{2+}, Mg^{2+}) + 7 O_2 + 70 H_2O = 28 Ep + 33.6 Na^+ + 39 SiO_2 + 112 H^+	+6	−14
5	56 Or + 33.6 Na^+ + 11 Ca^{2+} = 44.8 $Pl(An_{25})$ + 56 K^+ + 45 SiO_2	−9	−26
6	8 Bt + 53 $Pl(An_{100})$ + 28 SiO_2 + 35 Ca^{2+} + 49 H_2O + 5.5 O_2 = 44 Ep (Ps_{16}) + 8 Kfs + 70 H^+	−3	−
7	$Ca_2Al_2Si_3O_{12}(OH)$ = $CaAlSiO_4(OH)$ + $CaAl_2Si_2O_8$	+13	...

1. Reactions balanced on Al using representative but simplified results of electron-microprobe analyses in Table 3.
2. The percentage change in mineral volume of reaction considering all SiO_2 as quartz. Volume data from Table 3.
3. The percentage change in mineral volume of reaction considering all SiO_2 as being aqueous.

Epidote replacement of biotite is locally metasomatic, with Ca^{2+} imported and SiO_2 consumed. Balancing on Al_2O_3 for an epidote composition of 16 mole % and considering only the annite component of biotite, the reaction (number 6, Table 4) is:

biotite + plagioclase + quartz + H_2O + O_2 + Ca^{2+} = epidote + K-feldspar + H^+.

As written, the reaction is quite consistent with the textural associations observed. That is, the reactants quartz and plagioclase are not found with the biotite–epidote association, and apparently their consumption arrested the progress of reaction 6. This reaction is unique in these rocks in that it alone consumes quartz, as shown in Figures 7A and 7C. Here, reaction product K-feldspar is not associated with its coproduct, epidote. On the contrary, K-feldspar has invaded myrmekite from a former phenocryst replacement (reaction 5), and is replacing the included vermicular quartz (yellow arrows, Fig. 7B) at quartz–plagioclase interfaces. Some quartz grains are particularly scalloped (counterclockwise yellow arrow), further showing the direction of reaction. Thus, reaction 6 could be broken into two parts: epidote replacing biotite while releasing K^+, and K^+ + quartz + plagioclase replaced by K-feldspar, *i.e.*, a rare example of the reversal of the myrmekite producing reaction (reaction 5, Table 4).

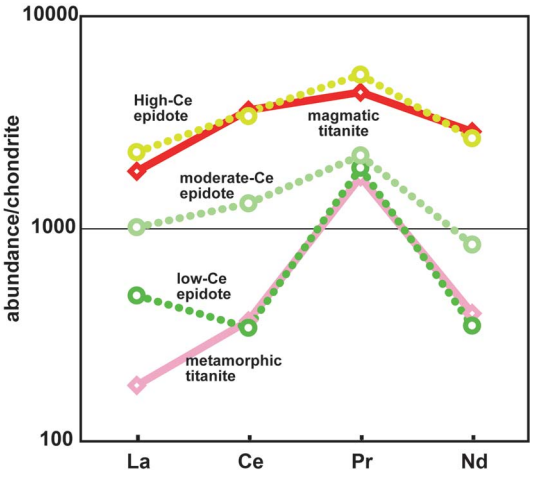

FIG. 9. A comparison of average compositions of epidote with low, intermediate, and high concentrations of rare earth elements with the compositions of magmatic and metamorphic titanite. Note that the high-Ce epidote contains the REE in the same concentrations as those present in the incompletely replaced magmatic titanite. This finding supports the interpretation that epidote precipitated while magmatic titanite dissolved.

Biotite–titanite intergrowths are common even where biotite is replaced by plagioclase. For example, the distribution of titanite along the boundaries and cleavages of biotite grains in Figure 3D suggests that titanite is a by-product of biotite replacement by plagioclase. Note especially the subhedral grains of titanite included in the lobate embayment of plagioclase (center left of the figure), suggesting the former presence of biotite along that trace. A likely reason for the local precipitation of titanite here and in intergrowths such as shown in Figure 7C is the low aqueous solubility of TiO_2, which retards its transport to other sites of precipitation.

Metasomatic replacement of magmatic titanite

A third example of metasomatic reaction involves the replacement of magmatic titanite. Magmatic titanite is relatively rich in REE, Y, and Fe^{3+} (Table 1) as well as U (Aleinikoff *et al.* 2002). Metamorphic titanite in these rocks contains much less of these elements, but more Al and Nb (Table 1, Figs. 5, 6, 8; Wintsch & Yi 2002). These minor and trace elements apparently made the composition of magmatic titanite metastable relative to epidote + metamorphic titanite. Evidence for this comes from the ubiquitous isolation of magmatic titanite by overgrowths of metamorphic titanite. The schematic reaction is:

magmatic titanite + Al^{3+} → metamorphic titanite + REE^{3+} + Fe^{3+}.

It is not an equilibrium but a description of the dissolution of the metastable magmatic titanite. Evidence for partial dissolution comes from the truncation of its oscillatory zoning patterns in the cores of titanite grains and the replacement by the overgrowing metamorphic titanite with completely different patterns of zoning (Figs. 4A, 8A). Metamorphic titanite also isolated magmatic titanite from metamorphic aqueous fluids, thus preventing further dissolution. Where grains were fractured, new metamorphic titanite healed the fracture (Aleinikoff *et al.* 2002), and also protected the grain from further dissolution.

Details of the reaction mechanism are further revealed by monitoring the concentrations of key trace elements in magmatic titanite. The REE in particular were not taken up in the solid solution of metamorphic titanite (Fig. 4D), but required an alternative host. We suggest that these liberated REE were precipitated as the allanite component of the adjacent metamorphic epidote. Evidence for the coprecipitation of epidote and titanite comes from the common association and intergrowth of these two minerals (Figs. 4, 8A). Moreover, the epidote grains show zoning defined by fluctuating REE contents. This is evident in back-scattered electron images, which show brighter bands where the REE content is relatively high (Fig. 4A), as confirmed

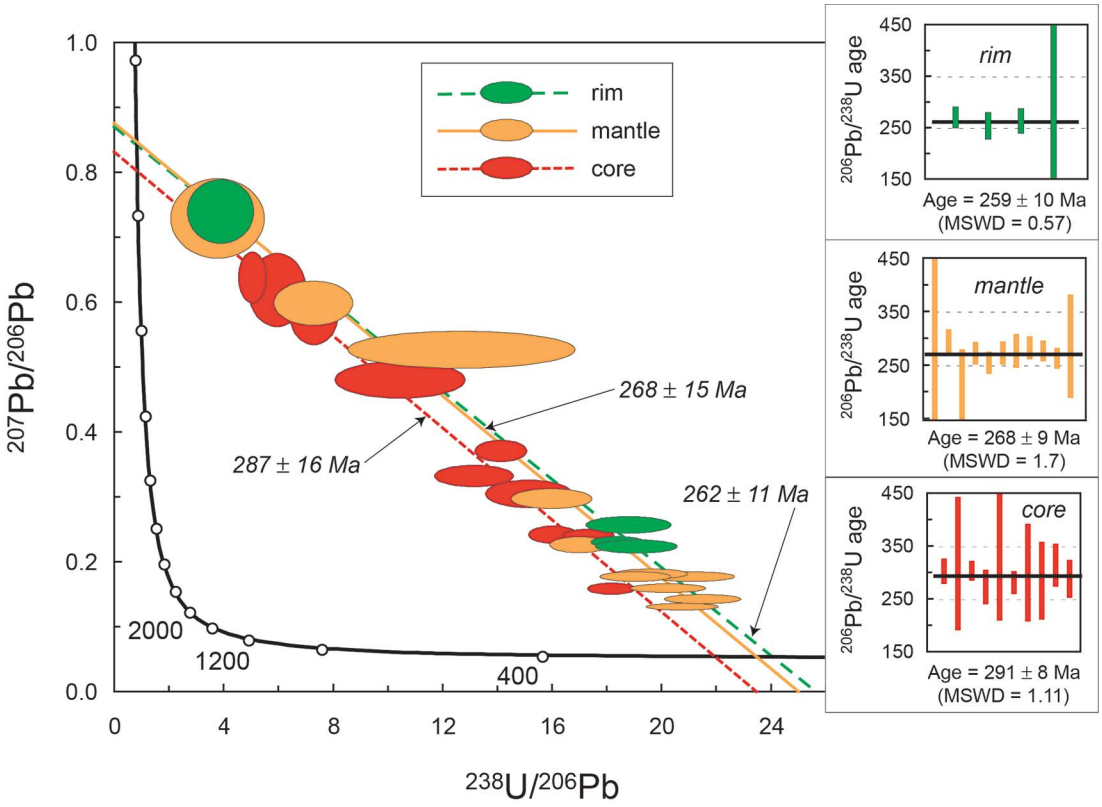

FIG. 10. A Tera–Wasserburg plot showing the regression of results of SHRIMP analyses of metamorphic titanite overgrown on both relict Ordovician magmatic grains and metamorphic cores (*e.g.*, Figs. 4, 8). The data are grouped into core, mantle, and rim compositions by independent microprobe identification of chemical zoning (Table 3, see text). Weighted averages of the $^{206}Pb/^{238}U$ ages are shown in the insets. The original data were described by Aleinikoff *et al.* (2002).

by element mapping (Fig. 4D). Finally, a qualitative mass-balance (Fig. 9) shows that the concentrations and distributions of light and intermediate REE in the REE-rich bands of epidote are indistinguishable from those in the magmatic titanite, suggesting that titanite was the source of the REE in the epidote. With this interpretation, we suggest that: (1) the epidote crystallized during the dissolution of magmatic titanite, and (2) the "mobility" of the REE in the presence of epidote is on the order of only hundreds of micrometers. The restriction of the REE to bands in epidote further suggests that the aqueous concentrations of the REE in the grain-boundary fluid were not uniform during the crystallization of epidote, but were available during relatively abrupt events involving the dissolution of magmatic titanite. These events may have been activated by deformation, which would have caused pressure solution and fracturing of magmatic titanite. Such processes have already been identified (Wintsch & Yi 2002), and make a good case for an inference that the dissolution of magmatic titanite was syntectonic, and that it occurred during fluctuating rates of extension during the 30 m.y. Alleghanian orogeny.

Driving mechanisms of reactions

Inspection of reaction 1 (Table 4) shows that (1) a metastable magmatic assemblage was partially replaced by a stable metamorphic assemblage, (2) the replacement involved hydration, requiring the introduction of H_2O and O_2-bearing fluids, and (3) the change in mineral volume of the reaction is –3%, such that it would be driven by an increase in pressure. The primary driving force for the reaction was undoubtedly the chemical metastability of the magmatic assemblage. However, the reaction could not have proceeded without the introduction of fluids. Fluids were available from below, because these orthogneisses were thrust over lower-grade pelitic rocks, causing prograde metamorphism and dehydration of the latter during the Alleghanian orogeny (Wintsch

et al. 2003). The H_2O evolved presumably infiltrated into these hanging-wall orthogneisses, providing the fluid necessary for reaction 1 to proceed. This process was assisted by the 3% volume loss associated with the operation of reaction 1, which would have increased the porosity and permeability of the rock, thus enhancing the development of pathways for the introduction of fluids.

Increasing pressure was also a factor. Wintsch *et al*. (2003) described structures showing that the Glastonbury complex was itself overridden, resulting in increased pressure, further contributing to driving reaction 1 to the right. Recognizing that SiO_2 did not precipitate locally as quartz at the reaction site, but as ribbons in microstructurally independent sites, then the ΔV_r of the metasomatic subreactions 2–5 became even more negative (Table 4). In this case, all four reactions show a strongly negative ΔV_r, and all four would be strongly favored by local high, normal stresses. It is thus not surprising that the strain accompanying these reactions would establish local pressure-gradients that would, in turn, drive the transport of aqueous SiO_2 toward extensional sites, where quartz precipitated as ribbons or even veins (Figs. 1–3, 7C). These were nourished by the SiO_2 released in each of the local replacement reactions (Fig. 12; see also Knipe & Wintsch 1985).

Reaction and rheology: evolution of the metamorphic fabric

The reactions described above had a significant effect on the strength of the orthogneiss, in part by reaction softening and reaction hardening. For example, reaction 1 moved to the right *via* a "Carmichael loop", such that not all the reactants and products crystallized together in a single microstructure. A calculation of the net changes in the volume of minerals in reaction 1 (Table 4) shows that 58% of the former volume of the amphibole is replaced by biotite. The biotite, in turn, contributed strongly to the foliation in the evolving orthogneiss. Thus reaction 1 weakened the rock not only by replacing the stronger amphibole with the weaker biotite, and thus increasing the phyllosilicate mode, but also by increasing the preferred orientation, and perhaps also the contiguity of biotite grains. The strain localization consequent to such weakening (Shea & Kronenberg 1993) would have provided an increasingly pervasive network of pathways for the easy infiltration of H_2O, and helped the overall hydration reaction to proceed.

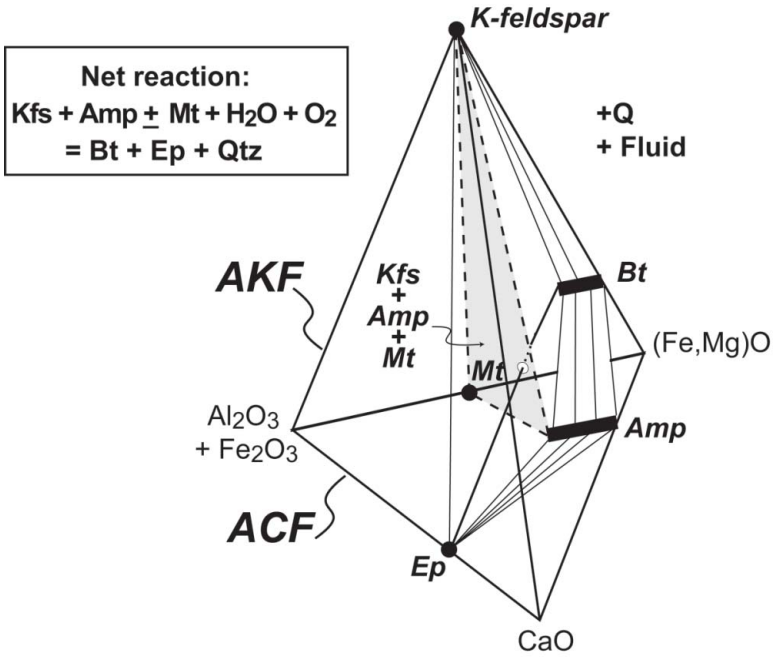

FIG. 11. A phase diagram produced by joining an ACF and an AKF diagram on their common Al – (Fe + Mg) base. The metastable assemblage of magmatic amphibole + K-feldspar + magnetite (shaded tie-plane) is cut by the stable biotite + epidote solid tie-line, showing the reaction relationship between the former reactants and the latter products.

Thus reaction 1 is an example of significant reaction softening.

Quartz is also a significant product of reaction in reactions 1–5 (Table 4). In fact, 21% by volume of the reactants of reaction 1 were replaced by quartz. Because quartz is also a relatively weak mineral, its addition to the mode will also contribute to weakening the rock. This is especially true because quartz tends to crystallize in ribbons and even as small veins where strain can also be localized, thereby avoiding the stronger amphibole-, feldspar-, and epidote-rich domains.

Reaction 6 (Table 4), involving the replacement of biotite + quartz by epidote and K-feldspar, is an example of reaction hardening. In this example, 26 volume % of the reactants are the weaker biotite + quartz. Thus from a modal standpoint, the assemblage is stronger. However, the crystallization of epidote *across* the foliae of biotite completely interrupts the contiguity of biotite (*e.g.*, Figs. 7A, C). This has the added influence of textural strengthening of the fabric. Thus reaction 6 in these rocks is an example of both modal and textural hardening.

In summary, the Glastonbury gneiss complex was considerably weakened by the operation of reaction 1 during prograde and high-grade metamorphism, by processes of both reaction softening and textural softening. It was later strengthened during retrograde metamorphism by the replacement of biotite and quartz by epidote (reaction 6) and by the disruption of biotite foliae. This strengthening constituted reaction and textural hardening.

Titanite as a metamorphic geochronometer

The presence of sufficient amounts of U in titanite make it a potentially powerful metamorphic geochronometer. Its relatively high closure-temperature to Pb diffusion mean that it will yield crystallization ages in all but the highest metamorphic grades (Frost *et al*. 2000). However, the ages are not easily interpreted unless the causes of titanite crystallization can be established. One way to establish its position in the metamorphic evolution of a rock is to take advantage of the time of crystallization produced by SHRIMP analysis. If the P–T–t path of metamorphism can be established by other means, then the age of crystallization can be used to ascertain the metamorphic conditions of that crystallization. Unfortunately, the lack of chemical equilibrium among all the phases in this orthogneiss, in addition to the low variance of the assemblage, do not allow the application of thermobarometry to define the metamorphic conditions of titanite crystallization.

As an alternative, the P–T–t path in these rocks has been established by one-dimensional inverse thermal modeling constrained by U–Pb crystallization ages, and $^{40}Ar/^{39}Ar$ cooling ages (Wintsch *et al.* 2003). The heating and cooling history of these rocks (Fig. 13A) can be described by the loading and unloading schedule of

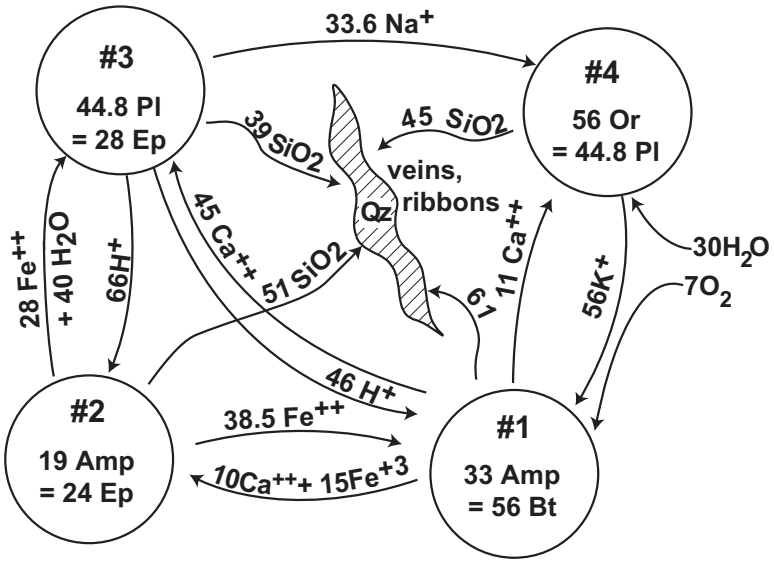

FIG. 12. A model for the metasomatic reactions occurring in the Glastonbury orthogneiss. All reactions (#1–4, Table 2) occur simultaneously such that the net reaction (#1, Table 4) is : amp + Kfs + H_2O + O_2 = bt + ep + qtz. Only H_2O and O_2 are introduced into the orthogneiss.

Figure 13B (bold blue line). Applying the ages of titanite cores, mantles, and rims to this temperature–time curve yields estimates of temperature and, through modeling, also pressures of crystallization. These conditions are more traditionally shown on the model P–T path of Figure 14. The ages of these zones thus clearly show the retrograde metamorphic conditions of their crystallization, during a significant decompression of these rocks.

In this regard, it is unexpected that the Al content of titanite should increase with decreasing pressure (Fig. 8), given the studies that suggest that Al content increases with high pressure (Frost *et al*. 2000, Troitzsch & Ellis 2002, Tropper *et al.*2002). One clue lies in the intergrowth of titanite with epidote (Fig. 4A). A reaction relationship exists between these two minerals, such that clinozoisite = anorthite + $CaAlSiO_4(OH)$, the Al–OH component of titanite (reaction 7, Table 4). The ΔV_r of this reaction as written is +13% , showing that the relative stability of the Al–OH component of titanite increases with decreasing pressure. Evidence for the operation of this reaction comes from the local truncation of zoning in the rims of epidote grains, indicating its resorption. In further support, the increase in Fe^{3+} content of epidote (Wintsch & Yi 2002) could reflect the loss of the clinozoisite component to the above reaction. The fluctuating increase in the An content of zoned plagioclase is also explained by the operation of this reaction. It is thus very likely that decompression contributed to the overgrowths of titanite in these rocks.

Two reactions that produce metamorphic titanite have been identified. One involves the dissolution of metastable magmatic titanite, whereas the other involves the replacement of biotite by titanite and epidote (Figs. 3D, 4, and 7). The ages of titanite crystallization may therefore record the times of dissolution of biotite or magmatic titanite, both of which are arguably

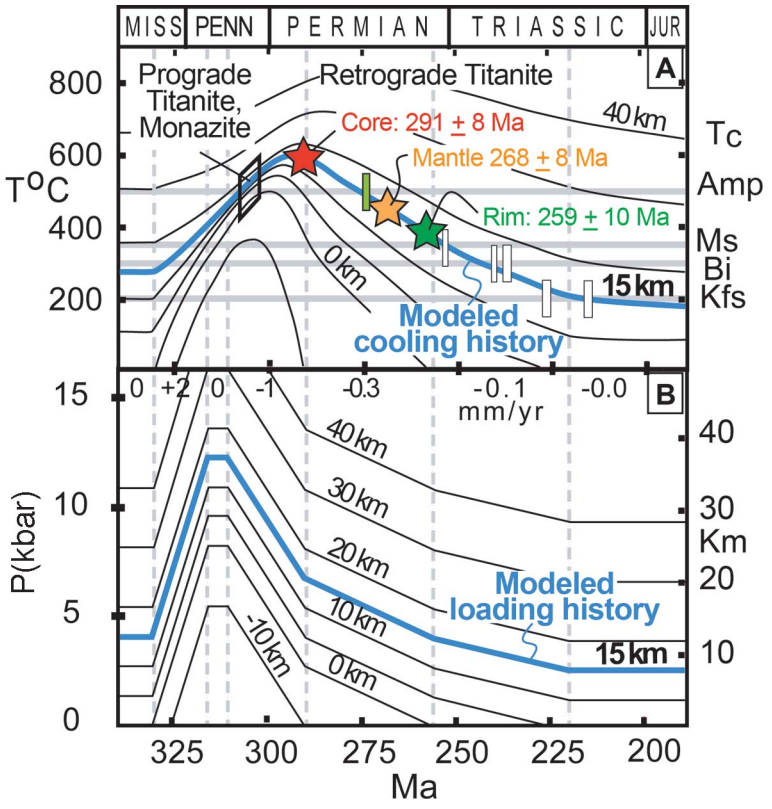

FIG. 13. The thermal and model loading histories of rocks in the southern Glastonbury complex, as defined by prograde titanite and monazite from Coleman *et al.* (1997), and by $^{40}Ar/^{39}Ar$ cooling ages of amphibole, muscovite, biotite, and K-feldspar plotted at their respective closure temperatures (Tc) (from Wintsch *et al.* 2003). Temperatures of crystallization of core, mantle, and rim regions of metamorphic titanite (stars) are established by the intersections of their ages (Fig. 10) with this temperature–time curve.

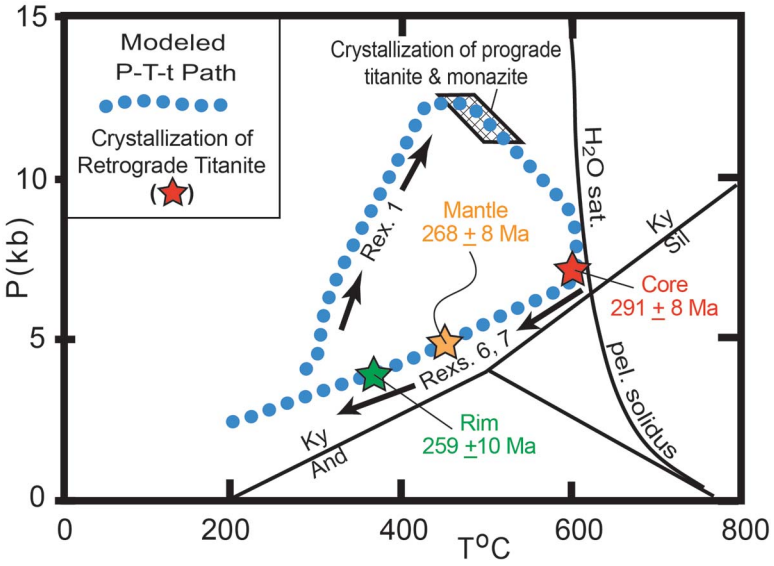

FIG. 14. The calculated P–T–t path of rocks of the southern Glastonbury complex (from Fig. 13). Reaction 1 (Rex 1) is believed to have been initiated during prograde metamorphism, and the replacement of biotite by epidote (Rex 6) occurred during the waning of metamorphic conditions. The retrograde P–T conditions of the crystallization of cores, mantles, and rims of metamorphic titanite (stars), probably in part *via* reaction 7, are established by their ages (Figs. 10, 13).

syntectonic. Thus ages of titanite crystallization may monitor the development of the foliation, or the localization of strain in this foliation, which occurred during retrograde metamorphic conditions.

Recrystallization of the metamorphic assemblage

Plagioclase is not predicted to be a reactant in reaction 1, but it clearly did participate. Given that the reactions are syntectonic, and that plagioclase appears to have dissolved and precipitated during pressure-solution creep processes (Wintsch & Yi 2002), *all* the minerals seem to be participating in the reaction process, each in its own reaction site. However, reaction progress is limited by the rate of dissolution of the magmatic reactants (amphibole, K-feldspar, and titanite). The significance of the dissolution rate of the reactants was noted by Carmichael (1979), who observed that the metastable persistence of some minerals also led to irregularly shaped isogradic surfaces. Deformation, and the strain energy it adds to a deforming rock (δw), can provide the activation energy for dissolution, as well as provide pathways for the introduction of aqueous fluids by which these reactions occur.

CONCLUSIONS

The mechanism of reaction during metamorphism of granodioritic orthogneiss is found to be one of dissolution of the metastable reactants and precipitation of stable products. Textural relationships suggest that metastable assemblages of K-feldspar + hastingsite ± magnetite are replaced by stable biotite + epidote + quartz in the presence of introduced H_2O and O_2. However, the local replacement-type reactions commonly involve only two of these minerals at any one replacement site. The specific replacement reactions deduced from these relationships reveal a family of open-system metasomatic reactions operating together in time, and nearby in space, but in domains not necessarily touching. Although plagioclase is not readily predicted as a reactant or product, it clearly participates in the reactions, especially in the replacement of K-feldspar and epidote.

Titanite is a significant, but volumetrically minor byproduct of the reaction. Its Alleghanian age established by the SHRIMP U–Pb method dates the time of its crystallization, and because the reactions were deformation-induced, also the time of these deformation events. A model P–T–t path shows that the crystallization

occurred during decompression, and electron-microprobe analyses demonstrate that the Al content of the grains increased from core to rim. This is explained by the large increase in volume of the reaction clinozoisite = plagioclase + Al-dominant titanite, the reaction believed to be responsible for the crystallization of retrograde titanite.

Deformation appears to have been critical in defining reaction progress in several ways. It produced pathways for the introduction of the fluids necessary to nourish the hydration reactions, and it provided the activation energy necessary for the aqueous dissolution of the metastable minerals. The reactions, in turn, provided a critical feedback, with their –3% reduction in volume contributing to the porosity and permeability that facilitated the introduction of fluids. The aqueous fluids were important because they are progress-limiting reactants. They also allowed the metastable minerals and assemblages to dissolve, and facilitated chemical communication among the local reaction-sites by providing a relatively rapid pathway for the transport of the ions dissolved. Finally, the reactions and development of fabric involved in the overall transformation of the Glastonbury granodiorite to an orthogneiss also contributed significantly to weakening the gneiss by reaction and textural softening. We suspect that dissolution – transportation – precipitation as a mechanism of reaction and deformation is widespread in most H_2O-bearing dynamic metamorphic environments.

Acknowledgements

We thank Dugald Carmichael for inspiring us to think flexibly about metamorphic reactions and processes. This work was originally presented at the 2003 GAC–MAC meeting honoring his career. We have benefitted from discussions and comments on earlier drafts with others, including M. Attenoukon, D. Bish, T. Byrne, D. Carmichael, A. Kronenberg, C. McWilliams, C. Simpson, and J. Urai. The formal reviews of N. Bégin, H. Day, G. Dipple, S. Johnson, R.F. Martin, and J. Selverstone contributed to the clarity of the final manuscript. This work was partially supported by NSF grants EAR–9418203 and EAR–9909410 to RPW.

References

Aleinikoff, J.N., Wintsch, R.P., Fanning, C.M. & Dorais, M.J. (2002): U–Pb geochronology of polygenetic sphene: an integrated SEM, EMPA, and SHRIMP study. *Chem. Geol. – Isotope Geosci.* **188**, 125-147.

Bestmann, M., Prior, D.J. & Veltkasmp, K.T.A. (2004): U–Pb development of single crystal s-shaped quartz porphyroclasts by dissolution–precipitation creep in a calcite marble shear zone. *J. Struct. Geol.* **26**, 869-883.

Bosworth, W. (1981): Strain enhanced dissolution of halite. *Tectonophysics* **78**, 509-525.

Brown, P.R.L. & Ellis, A.J. (1970): The Ohaki–Broadlands hydrothermal area, New Zealand: mineralogy and related geochemistry. *Am. J. Sci.* **269**, 97-131.

Carmichael, D.M. (1969): On the mechanism of prograde metamorphic reactions in quartz bearing pelitic rocks. *Contrib. Mineral. Petrol.* **20**, 244-267.

_____ (1979): Some implications of metamorphic reaction mechanisms for geothermobarometry based on solid-solution equilibria. *Geol. Soc. Am., Abstr. Programs* **11**, 398.

Coleman, M.E., Pulver, M.H., Byrne, T., Kiyokakaw, S., Wintsch, R., Davidek, K. & Martin, M. (1997): Late Paleozoic shortening and metamorphism within the Bronson Hill Terrane, central Connecticut. *Geol. Soc. Am., Abstr. Programs* **29**, 231.

Dahl, P.S. (1996): The effect of composition on retentivity of argon and oxygen in hornblende and related amphiboles: a field tested empirical model: *Geochim. Cosmochim. Acta* **60**, 3687-3700.

Engelder, T. (1982): A natural example of the simultaneous operation of free face dissolution and pressure solution. *Geochim. Cosmochim. Acta* **46**, 69-74.

Frost, B.R., Chamberlain, K.R. & Schumacher, J.C. (2000): Sphene (titanite): phase relations and role as a geochronometer. *Chem. Geol.* **172**, 131-148.

Imon, R., Okudaira, T. & Fujimoto, A. (2002): Dissolution and precipitation processes in deformed amphibolites: an example from the ductile shear zone of the Ryoke metamorphic belt, SW Japan. *J. Metamorph. Geol*. **20**, 297-308.

Knipe, R.J. & Wintsch, R.P. (1985): Heterogeneous deformation, foliation development and metamorphic processes in a polyphase mylonite. *In* Advances in Physical Geochemistry IV (A.B. Thompson & D.C. Rubie, eds.). Springer-Verlag, New York, N.Y. (180-210).

Leo, G.W., Zartman, R.E. & Brookins, D.G. (1984): Glastonbury gneiss and mantling rocks (a modified Oliverian dome) in south-central Massachusetts and north-central Connecticut: geochemistry, petrogenesis, and radiometric age. *U.S. Geol. Surv., Prof. Pap.* **1295**.

Merino, E. (1975): Diagenesis in Tertiary sandstones from Kettleman North dome, California. 1. Diagenetic mineralogy. *J. Sed. Petrol*. **45**, 320-336.

Milliken, K.L. (2003): Diagenesis. *In* Encyclopedia of Sediments and Sedimentary Rocks (G.V. Middleton, ed.). Kluwer, Dordrecht, The Netherlands (214-218).

Moench, R.H. & Aleinikoff, J.N. (2002): Stratigraphy, geochronology, and accretionary terrane settings of two Bronson Hill arc sequences, northern New England. *Phys. Chem. Earth* **27**, 47-95.

Pearce, T.H. & Kolisnik, A.M. (1990): Observations of plagioclase zoning using interference imaging. *Earth Sci. Rev*. **19**, 9-26.

SELVERSTONE, J. & HYATT, J. (2003): Chemical and physical responses to deformation in micaceous quartzites from the Tauern Window, Eastern Alps. *J. Metamorph. Geol.* **21**, 335-345.

SHEA, W.T., JR. & KRONENBERG, A.K. (1993): Strength and anisotropy of foliated rocks with varied mica contents. *J. Struct. Geol.* **15**, 1097-1121.

SIMPSON, C. & WINTSCH, R.P. (1989): Evidence for deformation-induced K-feldspar replacement by myrmekite. *J. Metamorph. Geol.* **7**, 261-275.

SMYTH, J.R., & BISH, D.L. (1988): *Crystal Structures and Cation Sites of the Rock-Forming Minerals*. Allen & Unwin, Boston, Massachusetts.

STOECKERT, B., WACHMANN, M., KUSTER, M. & BIMMERMANN, S. (1999): Low effective viscosity during high pressure metamorphism due to dissolution precipitation creep: the record of HP–LT metamorphic carbonates and siliciclastic rocks from Crete. *Tectonophysics* **303**, 299-319.

TROITZSCH, U. & ELLIS, D.J. (2002): Thermodynamic properties and stability of AlF-bearing titanite $CaTiOSiO_4$–$CaAlFSiO_4$. *Contrib. Mineral. Petrol.* **142**, 543-563.

TROPPER, P., MANNING, C.E. & ESSENE, E.J. (2002): The substitution of Al and F in titanite at high pressure and temperature: experimental constraints on phase relations and solid solution properties. *J. Petrol.* **43**, 1787-1814.

VERNON, R.H. (1986): K-feldspar megacrysts in granites; phenocrysts, not porphyroblasts. *Earth Sci. Rev.* **23**, 1-63.

WILLIAMS, M.L., SCHELTEMA, K.E. & JERCINOVIC, M.J. (2001): High-resolution compositional mapping of matrix phases; implications for mass transfer during crenulation cleavage development in the Moretown Formation, western Massachusetts. *J. Struct. Geol.* **23**, 923-939.

WINTSCH, R.P. & ANDREWS, M.S. (1988): Deformation induced growth of sillimanite: "stress" minerals revisited. *J. Geol.* **96**, 143-161.

_____, COLEMAN, M., PULVER, M., BYRNE, T., ALEINIKOFF, J.N., KUNK, M.J. & RODEN-TICE, M. (1998): Late Paleozoic deformation, metamorphism and exhumation in central Connecticut. *In* New England Intercollegiate Geologic Conference, Trip C2 (D.P. Murray, ed.). University of Rhode Island, Providence, Rhode Island (1–25).

_____ & DUNNING, J.D. (1985): The effect of dislocation density on the aqueous solubility of quartz and some geologic implications: a theoretical approach. *J. Geophys. Res.* **90**, 3,649-3,657.

_____, KUNK, M.J., BOYD, J.L. & ALEINIKOFF, J.N. (2003): P–T–t paths and differential Alleghanian loading and uplift of the Bronson Hill terrane, south-central New England. *Am. J. Sci.* **303**, 410-446.

_____ & YI, KEEWOOK (2002): Strain enhanced dissolution and replacement creep: a significant deformation mechanism in mid-crustal rocks. *J. Struct. Geol.* **24**, 1179-1193.

WONES. D.R. (1979): The fractional resorption of complex minerals and the formation of strongly femic alkaline rocks. *In* The Evolution of the Igneous Rocks, Fiftieth Anniversary Perspectives (H.S. Yoder Jr., ed.). Princeton Univ Press, Princeton, New Jersey (413-422).

Received October 19, 2003, revised manuscript accepted May 30, 2004.